Appl. Sci. **2015**, *5*, 1196-1210; doi:10.3390/app5041196

OPEN ACCESS

applied sciences

ISSN 2076-3417

www.mdpi.com/journal/applsci

Article

Polypropylene/Graphene and Polypropylene/Carbon Fiber Conductive Composites: Mechanical, Crystallization and Electromagnetic Properties

Chien-Lin Huang [1], Ching-Wen Lou [2], Chi-Fan Liu [3], Chen-Hung Huang [4], Xiao-Min Song [5] and Jia-Horng Lin [5,6,7,*]

1 Department of Fiber and Composite Materials, Feng Chia University, Taichung City 40724, Taiwan; E-Mail: clhuang@mail.fcu.edu.tw

2 Institute of Biomedical Engineering and Materials Science, Central Taiwan University of Science and Technology, Taichung City 40601, Taiwan; E-Mail: cwlou@ctust.edu.tw

3 Office of Physical Education and Sports Affairs, Feng Chia University, Taichung 407, Taiwan; E-Mail: cfliu@fcuoa.fcu.edu.tw

4 Department of Aerospace and Systems Engineering, Feng Chia University, Taichung City 40724, Taiwan; E-Mail: chhuang@fcu.edu.tw

5 Laboratory of Fiber Application and Manufacturing, Department of Fiber and Composite Materials, Feng Chia University, Taichung City 40724, Taiwan; E-Mail: sxm_1989@126.com

6 School of Chinese Medicine, China Medical University, Taichung City 40402, Taiwan

7 Department of Fashion Design, Asia University, Taichung City 41354, Taiwan

* Author to whom correspondence should be addressed; E-Mail: jhlin@fcu.edu.tw; Tel.: +886-4-2451-7250 (ext. 3405); Fax: +886-4-2451-0871.

Academic Editor: Wen-Hsiang Hsieh

Received: 23 September 2015 / Accepted: 30 October 2015 / Published: 13 November 2015

Abstract: This study aims to examine the properties of composites that different carbon materials with different measurements can reinforce. Using a melt compounding method, this study combines polypropylene (PP) and graphene nano-sheets (GNs) or carbon fiber (CF) to make PP/GNs and PP/CF conductive composites, respectively. The DSC results and optical microscopic observation show that both GNs and CF enable PP to crystalize at a high temperature. The tensile modulus of PP/GNs and PP/CF conductive composites remarkably increases as a result of the increasing content of conductive fillers. The tensile strength of the PP/GNs conductive composites is inversely proportional to the loading level of GNs. Containing 20 wt% of GNs, the PP/GNs conductive composites have an optimal

conductivity of 0.36 S/m and an optimal EMI SE of 13 dB. PP/CF conductive composites have an optimal conductivity of 10^{-6} S/m when composed of no less than 3 wt% of CF, and an optimal EMI SE of 25 dB when composed of 20 wt% of CF.

Keywords: polypropylene; graphene nano-sheets; carbon fibers; conducting composites; EMIs

1. Introduction

An intensively explored subject [1–12], polymer conductive composites are functional composites made by adding conductive fillers to polymers using a specified processing method, yielding steady and sustained electrical conductivity. Their electrical conductivity can also be adjusted with a greater range, and they are easily processed. Due to the aforementioned advantages, polymer conductive composites are commonly used in diverse fields, such as electronics, energy sources, and chemical engineering.

The electrical conductivity of polymer conductive composites is greatly dependent on the properties of the polymer as well as the conductive fillers' type, content, geometrical shape, and dispersion. The three major categories of conductive fillers are carbon, metal and metallic oxide, the former of which includes carbon black (CB) [5,13–16], carbon fibers (CF) [1,5,15,17–19], graphite [18,20,21], carbon nanotubes (CNT) [2,4,14,22,23], and grapheme [4,24–27] and is the most frequently used due to its light weight, its easy formation of conductive networks, and its oxidation resistance. Moreover, polymer conductive composites commonly use polypropylene (PP) [1,5,16,20], polyethylene (PE) [1,18], and polystyrene (PS) [3,13,16,24] as their matrices. PP is a highly commercially available polymer due to its excellent mechanical properties, good heat resistance, low cost, ease of processing, and full recyclability.

A melt compounding method is more appealing than an in-situ polymerization method or solution mixing method, and its combination of traditional facilities, such as an extruder and a mixer, can give the production a greater diversity of polymers and fillers. Such a method is relatively economical and suitable for mass production [28] and has already been successfully applied in the production of polymer conductive composites with the combination of conductive fillers of CNT, CB, expanded graphite, and grapheme [1,2,14,16,18]. With a melt compounding method, PP (*i.e.*, the matrix) is combined with GNs or CF (*i.e.*, conductive fillers) to form PP/GNs and PP/CF conductive composites. The crystallization properties, tensile properties, conductivity and EMI SE of the conductive composites are characterized by DSC, optical microscope observation, tensile test, conductivity test, and EMI SE test.

2. Experimental Section

2.1. Materials

PP (1080, Formosa Plastics Corporation, Taiwan) is a homopolymer with a density of 0.9 g/cm^3 and melt flow index of 10 g/10 min. CF (HTS 40, Toray Industries Inc., Tokyo, Japan) has a length of 6.2 mm and a diameter of 7 μm, as indicated in Figure 1a. GNs (Enerage Inc., Taiwan) have a thickness of 50–100 nm and a conductivity greater than 700 S/cm. The atomic force microscope (AFM) of GNs is indicated in Figure 1b.

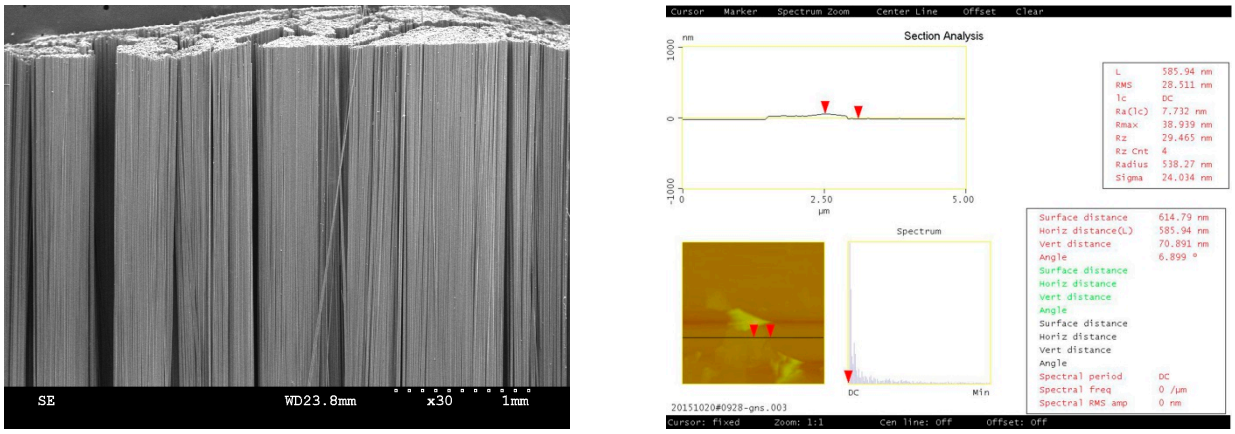

(a) **(b)**

Figure 1. (**a**) SEM image of CF (carbon fibers) and (**b**) AFM image of GNs (graphene nano-sheets).

2.2. Methods

PP/GNs and PP/CF conductive composites were made using a melt compounding method by a Brabender mixer with a processing temperature set to 180 °C, a processing time of 5 min, and a screw speed of 75 rpm. Finally, a hot press machine processed the conductive composites at 200 °C for 5 min to give them a 0.5-mm thickness, and cooled them at room temperature.

2.3. Tests

The conductive composites were evaluated by a differential scanning calorimeter (DSC), tensile test, flexural test, optical microscope observation, conductivity test, EMI SE test. In terms of the crystallization properties, DSC measurement used a Q200 (TA Instruments, New Castle, DE, USA) with samples that were heated from 40 °C to 200 °C at 10 °C/min increments, after which samples stayed at 200 °C for 5 min, then were cooled from 200 °C to 40 °C, and heated from 40 °C to 200 °C at the same increments. In terms of the mechanical properties, the tensile test was conducted according to ASTM D638. The optical microscopic observation was performed as follows. Tensile tests were performed via an Instron 5566 universal tester (Instron, Canton, MA, USA) as indicated in Figure 2, according to the specifications of ASTM D638-10. Samples were made into a dumbbell shape as seen in Figure 2c according to ASTM D638 Type IV. The crosshead speed was 5 mm/min and a total of five samples for each specification were used. A glass cover extended the samples into euphotic film at 200 °C on a specimen heating holder, and then each was placed in the optical microscope, isothermally cooled to 130 °C at 10 °C/min increments and kept at 130 °C so as to observe the crystallinity of PP. The conductivity of the conductive composites was evaluated by the four-point probe method, while the EMI SE of the samples was measured at a frequency range of 300 MHz to 3 GHz as specified in ASTM D4935.

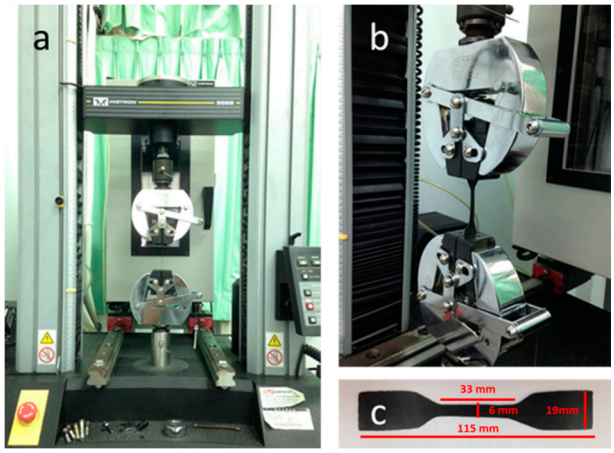

Figure 2. (**a**) The tester, (**b**) the grips, and (**c**) the samples of tensile tests.

3. Results and Discussion

3.1. Performance of Crystallization

Tables 1 and 2 show that PP has an initial crystallinity temperature (T_{onset}) of 116.21 °C and crystallinity temperature (T_c) of 111.46 °C, both of which shift to the high temperature zone as a result of the combination of GNs and also continuously increase as a result of the increasing content of GNs. The optimal T_{onset} of 140.67 °C and T_c of 135.01 °C are present when the PP/GNs conductive composites consist of 20 wt% of GNs, and are greater than those of pure PP by 24.46 °C and 23.55 °C, respectively. Similarly, T_{onset} and T_c of PP/CF conductive composites also shift to the high temperature zone as a result of the combination of CF, and also increase with the increasing levels of CF. When containing 20 wt% CF, PP/CF conductive composites have optimal T_{onset} (126.25 °C) and T_c (122.28 °C), which are greater than those of pure PP by 10.04 °C and 10.82 °C, respectively. Such results are ascribed to the combination of GNs or CF as the nucleating agent of PP, which makes the nucleation mode heterogeneous instead of homogeneous, significantly decreases the nucleation free energy, and allows the molecular chain to attach to and be arranged orderly on the nucleating agent [22,23]. GNs demonstrate a more significant influence over the T_{onset} and T_c of PP than CF does. Such a result is ascribed to the nanometer size effect of GNs, namely that the size of GNs is smaller than that of CF. With the same content, GNs contribute to a greater superficial area and at the same time greater nucleation sites, thereby demonstrating a greater effect on the T_{onset} and T_c of PP.

PP has T_{onset}–T_c of 4.75 °C and $t_{1/2}$ of 0.444 min. The combination of GNs results in a decrease in crystallization rate of PP, exemplified by an increase in T_{onse}–T_c of 4.79 °C to 6.1 °C and an increase in $t_{1/2}$ of 0.477 min to 0.604 min. By contrast, 15 wt% of GNs makes for the slowest crystallization rate of PP, making T_{onset}–T_c 6.10 °C and $t_{1/2}$ 0.604 min. Conversely, the combination of CF accelerates the crystallization rate of PP, causing T_{onset}–T_c to decrease to 3.70 °C–4.33 °C and $t_{1/2}$ to decrease to 0.358 min–0.443 min. In particular, 5 wt% of CF results in the shortest crystallization rate of PP, in which T_{onset}–T_c is 3.70 °C and $t_{1/2}$ is 0.358 min. The combination of inorganic fillers to polymers has two influences over the crystallization behavior of the polymer. Using inorganic fillers as nucleating agent allows the molecular chains of PP to nucleate and the spherocrystals to enlarge at a high temperature, and at the same time allows for more nucleation sites [24–29]. On the other hand, the existence of

inorganic fillers takes up a certain space, especially with nano-scale fillers, and restricts the motion and arrangement of molecular chains that influence the crystallization rate of the polymer. As a result, the crystallization rate of the polymer is inversely proportional to the inorganic fillers, but the combination of CF is proportional to the crystallization rate of PP.

The degree of crystallinity (X_c) of PP decreases slightly when the combination of GNs is below 5 wt%, and slightly increases when the combination of GNs is above 5 wt%. Conversely, the combination of CF hardly influences the X_c of PP.

Table 1. Crystallization properties of PP/GNs composites.

wt%	T_c (°C)	T_{onset} (°C)	T_{onset}–T_c (°C)	$t_{1/2}$ (min)	X_c (%)
0	111.46	116.21	4.75	0.444	40.3
1	124.91	129.70	4.79	0.479	38.6
3	127.54	132.43	4.89	0.477	38.6
5	129.39	135.22	5.83	0.567	45.1
10	132.75	138.19	5.44	0.543	44.5
15	133.36	139.46	6.10	0.604	45.7
20	135.01	140.67	5.66	0.574	45.4

Table 2. Crystallization properties of PP/CF composites.

wt%	T_c (°C)	T_{onset} (°C)	T_{onset}–T_c (°C)	$t_{1/2}$ (min)	X_c (%)
0	111.46	116.21	4.75	0.444	40.3
1	118.92	122.73	3.81	0.373	38.9
3	119.42	123.27	3.85	0.368	39.6
5	120.23	123.93	3.70	0.358	39.9
10	120.61	124.56	3.95	0.403	40.4
15	120.90	125.23	4.33	0.443	41.8
20	122.28	126.25	3.97	0.387	41.1

Figure 3 shows the image series occurring during the process that GNs are added to PP, and cooled from a melted state at 200 °C at 10 °C/min increments until it reaches 130 °C, where it is kept. The presence of GNs can be seen in the melted state image in Figure 3a. Figure 3b is the image photographed close to 130 °C, at which point the molecules start to nucleate and PP starts to nucleate the surrounding GNs. Figure 3c,d show that the spherocrystals continuously enlarge. Due to the nano-scale that GNs are at, the combination of GNs results in numerous nucleating sites in PP. Therefore, there is a great amount of spherocrystals of PP, which easily collide with adjacent spherocrystals, and as a result, spherocrystals have a small size and low completeness.

Figure 4 shows the image series occurring during the process in which CF was added to PP and cooled from a melted state at 200 °C at 10 °C/min increments until it reached 130 °C, where it was kept. The black part shown in Figure 4a is CF; Figure 4b shows that the molecular chains of PP nucleate and the spherocrystals enlarge along the CF; Figure 4c,d shows ever-growing spherocrystals and a clear transcrystallization. Compared to the combination of GNs, the combination of CF makes spherocrystals larger and more complete.

Figures 3 and 4 show that using GNs or CF as the nucleating agent facilitates the crystallization of PP. The combination of GNs results in a smaller spherocrystal size but a poorer completeness. Conversely, the combination of CF results in a larger spherocrystal size but a better completeness.

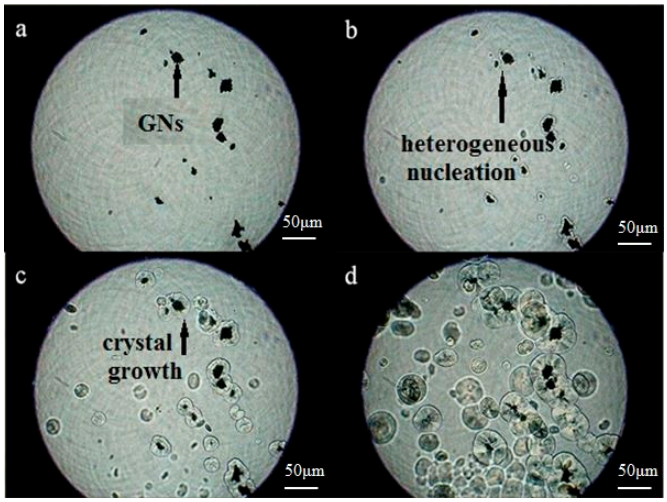

Figure 3. Optical microscopic images (500×) of PP/GNs composites at (**a**) 200 °C and (**b**–**d**) near 130 °C.

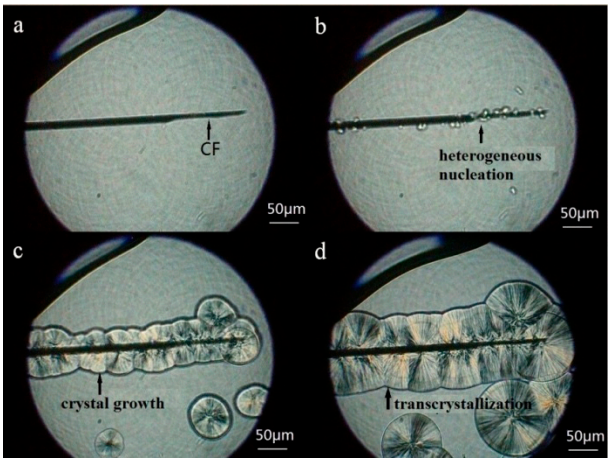

Figure 4. Optical microscopic images (500×) of PP/CF composites at (**a**) 200 °C and (**b**–**d**) near 130 °C.

3.2. Performance of Tensile Properties

The mechanical properties of polymer composites are highly correlated with the intrinsic properties, amount, dispersion of the fillers, the properties of the polymer matrix, and the interaction between fillers and polymer matrix. Figure 5 and Table 3 indicate the significant influence of the loading level of GNs over the mechanical properties of PP/GNs conductive composites and show that it is inversely proportional to the tensile strength but proportional to the tensile modulus. Compared to the mechanical properties of pure PP, the PP/GNs conductive composites containing 20 wt% of GNs have a 34% lower tensile strength (from 33.74 MPa to 22.28 MPa) and a 150% greater tensile modulus (from 1621 MPa *vs.* 4037 MPa).

In the tensile test, the fracture mode of PP is ductile fracture, which is quite different from that of PP/GNs conductive composites, which have an obvious yield phenomenon before fracture. Furthermore, when containing more content of GNs, PP/GNs conductive composites exhibit a classical brittle fracture, namely they do not exhibit a significant yield phenomenon before fracture. Additionally, their elongation at break is considerably low [30,31] as indicated in Figure 7a. GNs create a discontinuity of PP in PP/GNs conductive composites, and at the same time create a stress concentration phenomenon. When the composites are posed with load, the initial cracking occurs and then becomes worse where the stress concentration occurs, and eventually causes structural failure. Although serving as the dispersed phase, GNs are actually isolated from the PP matrix in the PP continuous phase, and resemble a sea-island structure. An increasing content of GNs inevitably decreases the force bearing area of matrix, thereby decreasing the tensile strength of the composites in comparison to that of pure PP. In addition, the conductivity of GNs stems from their own sp^2 hybridization structure; therefore, adding functional groups to GNs certainly destroys such a structure and then decreases GNs' initial conductivity. This study does not functionally modify GNs as it aims to develop polymer conductive composites with better conductivity. The modulus of the polymer composites can be augmented by adding fillers that have a high modulus to polymers that have a lower modulus, regardless of the interaction between them. Such a result is ascribed to a complex explanation, which is beyond any complete theories but it can be simply put that the fillers possess a restrictive effect over the polymers by restricting the motion and deformation of their molecular chains.

Figure 6 and Table 3 show that the increasing content of CF significantly influences the mechanical properties of the PP/CF conductive composites with their tensile strength first decreasing then increasing and the tensile modulus constantly increasing. Compared to the tensile strength (33.74 MPa) and modulus (1621 MPa) of pure PP, the combination of 20 wt% of CF causes the tensile strength of the PP/CF conductive composites to decrease by 8.3% to 30.94 MPa and increases their tensile modulus by 159% to 4207 MPa.

The combination of CF has a similar augmentation of the modulus to the combination of GNs. The PP/CF conductive composites do not exhibit an obvious yield phenomenon before fracture (*i.e.*, classical brittle fracture), and also have a remarkably low elongation at break [30,31], as indicated in Figure 7b. However, this elongation is still relatively greater than that of PP/GNs conductive composites. The increase in tensile modulus and the decrease in tensile strength of PP/CF conductive composites are caused by the same factors as that for PP/GNs conductive composites. When the content of CF is more than 3 wt%, the tensile strength of PP/CF conductive composites continuously increases, the result of which is ascribed to the cross structure caused by PP and a high content of CF. Some fibers are entangled and then provide the reinforcing effect, which is conducive to the tensile strength.

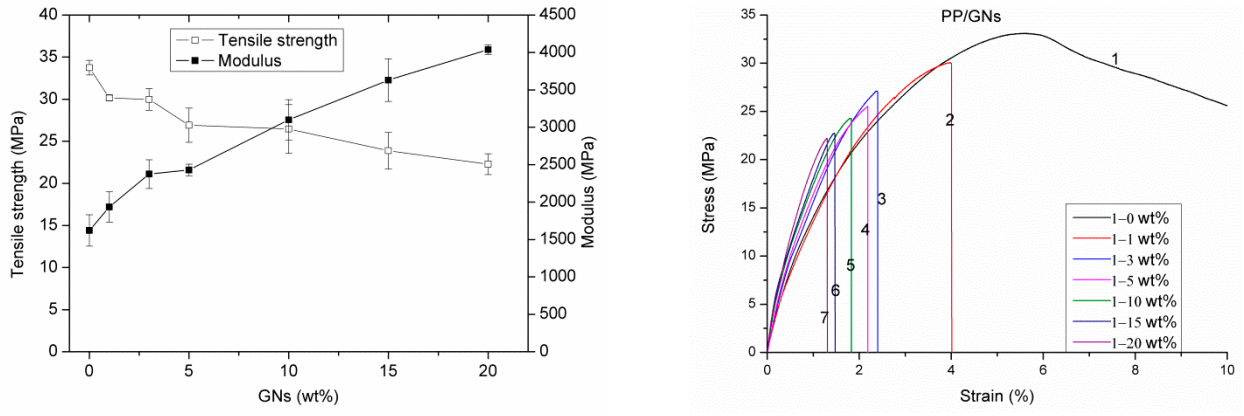

(**a**) (**b**)

Figure 5. The tensile properties of PP/GNs composites: (**a**) tensile strength and modulus and (**b**) stress-strain curve.

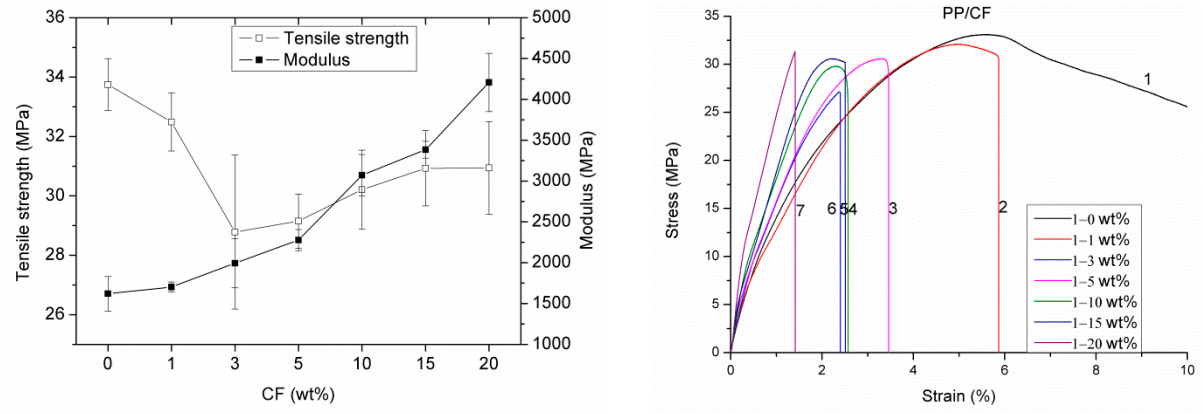

(**a**) (**b**)

Figure 6. The tensile properties of PP/CF composites: (**a**) tensile strength and modulus and (**b**) stress-strain curve.

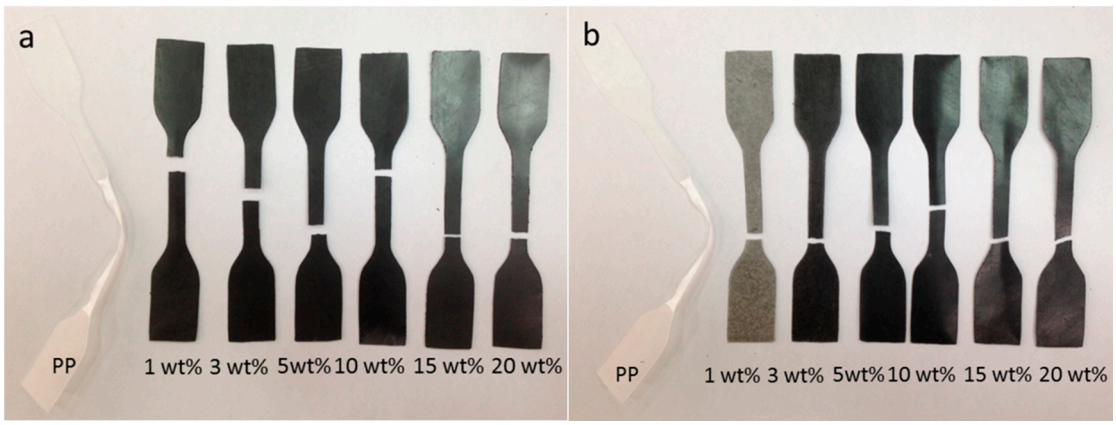

Figure 7. Stereomicroscopic images of the fractured samples: (**a**) PP/GNs composite and (**b**) PP/CF composites.

Table 3. Tensile properties and electrical conductivity of PP/GNs and PP/CF composites.

Filler (wt%)	GNs				CF			
	Tensile strength (MPa)	**Tensile Modulus (MPa)**	**Elongation (%)**	**Conductivity (S/m)**	**Tensile strength (MPa)**	**Tensile Modulus (MPa)**	**Elongation (%)**	**Conductivity (S/m)**
0	33.75 ± 0.87	1621 ± 211	>100	$1.2 \times 10^{-13} \pm 1.1 \times 10^{-13}$	33.75 ± 0.87	1621 ± 211	>100	$1.2 \times 10^{-13} \pm 1.1 \times 10^{-13}$
1	30.16 ± 0.34	1934 ± 203	3.66 ± 0.75	$9.2 \times 10^{-10} \pm 2.4 \times 10^{-10}$	32.49 ± 0.98	1703 ± 60	5.75 ± 0.5	$3.4 \times 10^{-6} \pm 1.2 \times 10^{-6}$
3	29.98 ± 1.29	2374 ± 192	3.07 ± 0.33	$6.8 \times 10^{-10} \pm 1.3 \times 10^{-10}$	28.78 ± 2.59	1993 ± 301	2.64 ± 0.36	$3.8 \times 10^{-6} \pm 1.4 \times 10^{-6}$
5	26.92 ± 2.03	2429 ± 78	2.63 ± 0.39	$2.3 \times 10^{-5} \pm 1.2 \times 10^{-5}$	29.15 ± 0.91	2278 ± 129	3.54 ± 0.26	$3.8 \times 10^{-6} \pm 1.3 \times 10^{-6}$
10	26.46 ± 2.89	3099 ± 270	1.86 ± 0.15	$1.1 \times 10^{-2} \pm 0.003$	30.22 ± 1.33	3072 ± 252	2.59 ± 0.16	$3.1 \times 10^{-6} \pm 1.1 \times 10^{-6}$
15	23.88 ± 2.17	3630 ± 280	1.54 ± 0.16	0.12 ± 0.01	30.94 ± 1.27	3384 ± 102	2.57 ± 013	$3.2 \times 10^{-6} \pm 1.2 \times 10^{-6}$
20	22.28 ± 1.23	4037 ± 64	1.21 ± 0.21	0.36 ± 0.12	30.95 ± 1.56	4207 ± 357	1.62 ± 0.23	$3.2 \times 10^{-6} \pm 1.3 \times 10^{-6}$

3.3. Performance of Electrical Conductivity and EMI SE

Figure 8 shows that the conductivity of pure PP is 10^{-13} S/m (*i.e.*, the orders of magnitude), which shows the classical insulating property of polymer. The combination of 5 wt% of GNs results in an increase of several orders of magnitude in the PP/GNs conductive composites, reaching 10^{-6} S/m, which indicates that the conductive composites have the percolation phenomenon; namely, a conductive network is formed between the conductive fillers. According to the percolation theory, the percolation threshold of PP/GNs conductive composites is 2.8 vol%. An increasing content of GNs results in a more complete conductive network and a greater conductivity. When combined with 20 wt% of GNs, the conductivity of PP/GNs conductive composites reaches 0.36 S/m. Figure 9 shows that PP/CF conductive composites containing 3 wt% of CF have a conductivity of 10^{-6} S/m. Moreover, the conductivity constantly retains the same regardless of the increasing content of CF. Such results are likely due to the initial properties of CF.

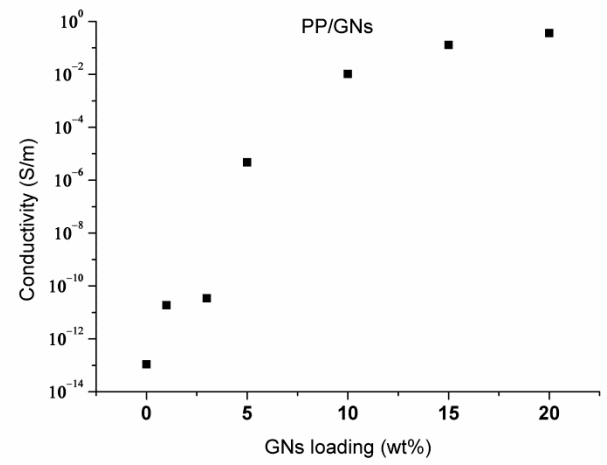

Figure 8. Conductivity of PP/ GNs composites as related to various blending ratios.

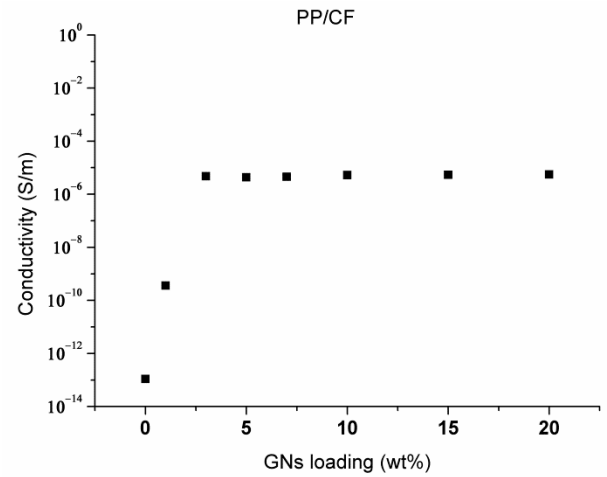

Figure 9. Conductivity of PP/ CF composites as related to various blending ratios.

The EMI SE of polymer conductive composites is correlated with factors such as the electrical conductivity and magnetic conductivity of composites, the thickness and geometry of shield, frequency, the distance between the shield and the field source, and the dispersion of the conductive fillers in

composites. Figures 10 and 11 show the EMI SE of the polymer conductive composites containing different contents of GNs or CF, respectively. The EMI SE of the polymer conductive composites increases as a result of an increasing content of GNs or CF. Due to an increase in fillers, the conductivity of the polymer conductive composites increases, which in turn augments their EMI SE [32–42]. At some specified frequencies, the EMI SE appears to be really high, and the extremum value of both PP/GNs and PP/CF conductive composites occur at a similar frequency, which is surmised to be determined by the initial properties of fillers belonging to the carbon category [18,43].

Figures 8 and 9 show that with the same loading level that is more than 5 wt%, the conductivity of PP/GNs conductive composites is greater than that of PP/CF conductive composites. However, the EMI SE of the PP/CF conductive composites is greater than that of the PP/GNs conductive composites as seen in Figures 10 and 11. In sum, the EMI SE of a shield is correlated with not only its conductivity, but also its initial properties.

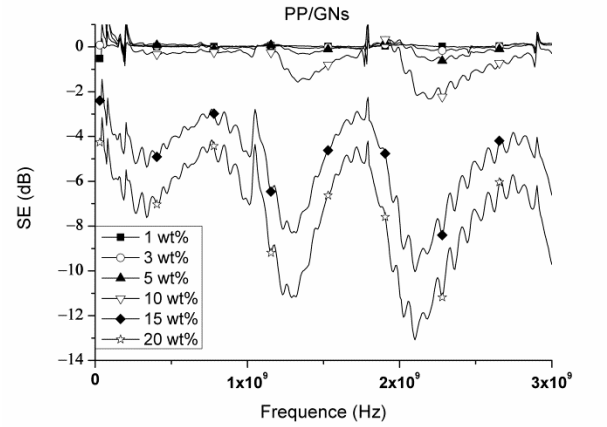

Figure 10. EMI SE of PP/GNs composites with a thickness of 0.5 mm as related to various blending ratios.

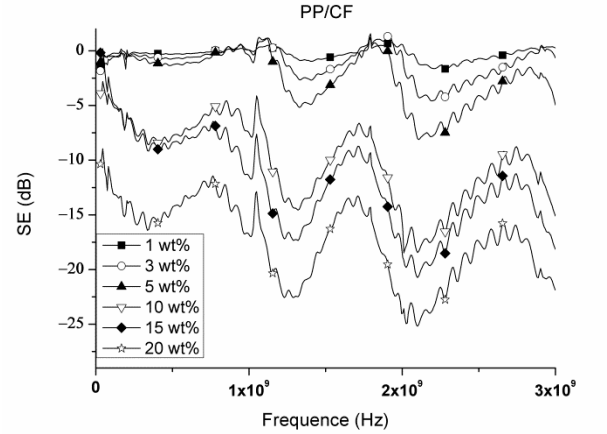

Figure 11. EMI SE of PP/CF composites with a thickness of 0.5 mm as related to various blending ratios.

4. Conclusions

This study successfully produces PP/GNs and PP/CF conductive composites by cooperating with a melt compounding method. The combination of these two filler types as the nucleating agent results in a greater crystallization temperature of PP. With the same content, GNs demonstrate a greater influence over the crystallization temperature than CF does. The combination of GNs retards the crystallization rate of PP, while the combination of CF does the opposite. The tensile modulus of both PP/GNs and PP/CF conductive composites is considerably proportional to the loading level of the conductive fillers. The tensile strength of PP/GNs conductive composites decreases with an increasing content of GNs, while that of PP/CF conductive composites first decreases then increases as a result of the increasing CF. The optimal conductivity of 0.36 S/m and the optimal EMI SE of 13 dB occurs when the PP/GNs conductive composites contain 20 wt% of GNs. By contrast, the optimal conductivity of 10^{-6} S/m occurs when the PP/CF conductive composites contain more than 3 wt% of CF, while the optimal EMI SE occurs when containing 20 wt% of CF. Therefore, possible applications in domestic appliances of the composites in terms of electrical and mechanical properties can thus be attained by adjusting different fillers and different amounts of them.

Acknowledgments

The authors would especially like to thank Ministry of Science and Technology of Taiwan, for financially supporting this research under Contract MOST 103-2221-E-035-027.

Author Contributions

In this study, the concepts and designs for the experiment, all required materials, as well as processing and assessment instrument are provided by Jia-Horng Lin and Ching-Wen Lou. Data are analyzed, and experimental results are examined by Chen-Hung Huang, Chien-Lin Huang, and Chi-Fan Liu. The experiment is conducted and the text is composed by Xiao-Min Song.

Conflicts of Interest

The authors declare no conflict of interest.

References

1. Shen, L.; Wang, F.Q.; Yang, H.; Meng, Q.R. The combined effects of carbon black and carbon fiber on the electrical properties of composites based on polyethylene or polyethylene/polypropylene blend. *Polym. Test.* **2011**, *30*, 442–448.
2. Huang, J.; Mao, C.; Zhu, Y.; Jiang, W.; Yang, X. Control of carbon nanotubes at the interface of a co-continuous immiscible polymer blend to fabricate conductive composites with ultralow percolation thresholds. *Carbon* **2014**, *73*, 267–274.
3. Shrivastava, N.K.; Khatua, B.B. Development of electrical conductivity with minimum possible percolation threshold in multi-wall carbon nanotube/polystyrene composites. *Carbon* **2011**, *49*, 4571–4579.

4. Chen, Y.-J.; Dung, N.D.; Li, Y.-A.; Yip, M.-C.; Hsu, W.-K.; Tai, N.-H. Investigation of the electric conductivity and the electromagnetic interference shielding efficiency of SWCNTs/GNS/PAni nanocomposites. *Diamond Relat. Mater.* **2011**, *20*, 1183–1187.
5. Zhao, S.; Zhao, H.; Li, G.; Dai, K.; Zheng, G.; Liu, C.; Shen, C. Synergistic effect of carbon fibers on the conductive properties of a segregated carbon black/polypropylene composite. *Mater. Lett.* **2014**, *129*, 72–75.
6. Calberg, C.; Blacher, S.; Gubbels, F.; Brouers, F.; Deltour, R.; Jerome, R. Electrical and dielectric properties of carbon black filled co-continuous two-phase polymer blends. *J. Phys. D* **1999**, *32*, 1517–1525.
7. Wen, M.; Sun, X.; Su, L.; Shen, J.; Li, J.; Guo, S. The electrical conductivity of carbon nanotube/carbon black/polypropylene composites prepared through multistage stretching extrusion. *Polymer* **2012**, *53*, 1602–1610.
8. Drubetski, M.; Siegmann, A.; Narkis, M. Electrical properties of hybrid carbon black/carbon fiber polypropylene composites. *J. Mater. Sci.* **2006**, *42*, 1–8.
9. Straat, M.; Boldizar, A.; Rigdahl, M.; Hagstrom, B. Improvement of melt spinning properties and conductivity of immiscible polypropylene/polystyrene blends containing carbon black by addition of styrene-ethylene-butene-styrene block copolymer. *Polym. Eng. Sci.* **2011**, *51*, 1165–1169.
10. Pramanik, P.K.; Khastgir, D.; Saharu, T.N. Conductive nitrile rubber composite containing carbon fillers: Studies on mechanical properties and electrical conductive. *Composites* **1992**, *23*, 183–191.
11. Thongruang, W.; Spontak, R.J.; Balik, C.M. Correlated electrical conductivity and mechanical property analysis of high-density polyethylene filled with graphite and carbon fiber. *Polymer* **2002**, *43*, 2279–2286.
12. Xu, H.-P.; Dang, Z.-M. Electrical property and microstructure analysis of poly(vinylidene fluoride)-based composites with different conducting fillers. *Chem. Phys. Lett.* **2007**, *438*, 196–202.
13. Kalaitzidou, K.; Fukushima, H.; Drzal, L.T. A new compounding method for exfoliated graphite–polypropylene nanocomposites with enhanced flexural properties and lower percolation threshold. *Compos. Sci. Technol.* **2007**, *67*, 2045–2051.
14. Sengupta, R.; Bhattacharya, M.; Bandyopadhyay, S.; Bhowmick, A.K. A review on the mechanical and electrical properties of graphite and modified graphite reinforced polymer composites. *Prog. Polym. Sci.* **2011**, *36*, 638–670.
15. McLachlan, D.S.; Chiteme, C.; Park, C.; Wise, K.E.; Lowther, S.E.; Lillehei, P.T.; Siochi, E.J.; Harrison, J.S. AC and DC percolative conductivity of single wall carbon nanotube polymer composites. *J. Polym. Sci., Part B: Polym. Phys.* **2005**, *43*, 3273–3287.
16. Miyazaki, K.; Okazaki, N.; Nakatani, H. Improvement of electrical conductivity with phase-separation in polyolefin/multiwall carbon nanotube/polyethylene oxide composites. *J. Appl. Polym. Sci.* **2013**, *128*, 3751–3757.
17. Stankovich, S.; Dikin, D.A.; Dommett, G.H.; Kohlhaas, K.M.; Zimney, E.J.; Stach, E.A.; Piner, R.D.; Nguyen, S.T.; Ruoff, R.S. Graphene-based composite materials. *Nature* **2006**, *442*, 282–286.
18. Potts, J.R.; Dreyer, D.R.; Bielawski, C.W.; Ruoff, R.S. Graphene-based polymer nanocomposites. *Polymer* **2011**, *52*, 5–25.
19. Geim, A.K.; Novoselov, K.S. The rise of graphene. *Nat. Mater.* **2007**, *6*, 183–191.

20. Hsiao, S.-T.; Ma, C.-C.M.; Tien, H.-W.; Liao, W.-H.; Wang, Y.-S.; Li, S.-M.; Huang, Y.-C. Using a non-covalent modification to prepare a high electromagnetic interference shielding performance graphene nanosheet/water-borne polyurethane composite. *Carbon* **2013**, *60*, 57–66.
21. Zhang, H.-B.; Zheng, W.-G.; Yan, Q.; Yang, Y.; Wang, J.-W.; Lu, Z.-H.; Ji, G.-Y.; Yu, Z.-Z. Electrically conductive polyethylene terephthalate/graphene nanocomposites prepared by melt compounding. *Polymer* **2010**, *51*, 1191–1196.
22. Lin, Y.; Chen, H.; Chan, C.M.; Wu, J. Nucleating effect of calcium stearate coated $CaCO_3$ nanoparticles on polypropylene. *J. Colloid Interface Sci.* **2011**, *354*, 570–576.
23. Sui, G.; Fuqua, M.A.; Ulven, C.A.; Zhong, W.H. A plant fiber reinforced polymer composite prepared by a twin-screw extruder. *Bioresour. Technol.* **2009**, *100*, 1246–1251.
24. Gao, Y.; Wang, Y.; Shi, J.; Bai, H.; Song, B. Functionalized multi-walled carbon nanotubes improve nonisothermal crystallization of poly(ethylene terephthalate). *Polym. Test.* **2008**, *27*, 179–188.
25. Xu, Y.; Shang, S.; Huang, J. Crystallization behavior of poly(trimethylene terephthalate)-poly(ethylene glycol) segmented copolyesters/multi-walled carbon nanotube nanocomposites. *Polym. Test.* **2010**, *29*, 1007–1013.
26. Ke, K.; Wang, Y.; Yang, W.; Xie, B.-H.; Yang, M.-B. Crystallization and reinforcement of poly (vinylidene fluoride) nanocomposites: Role of high molecular weight resin and carbon nanotubes. *Polym. Test.* **2012**, *31*, 117–126.
27. Xu, D.; Wang, Z. Role of multi-wall carbon nanotube network in composites to crystallization of isotactic polypropylene matrix. *Polymer* **2008**, *49*, 330–338.
28. Razavi-Nouri, M.; Ghorbanzadeh-Ahangari, M.; Fereidoon, A.; Jahanshahi, M. Effect of carbon nanotubes content on crystallization kinetics and morphology of polypropylene. *Polym. Test.* **2009**, *28*, 46–52.
29. Zhao, S.; Chen, F.; Huang, Y.; Dong, J.-Y.; Han, C.C. Crystallization behaviors in the isotactic polypropylene/graphene composites. *Polymer* **2014**, *55*, 4125–4135.
30. Korayem, A.H.; Barati, M.R.; Simon, G.P.; Zhao, X.L.; Duan, W.H. Reinforcing brittle and ductile epoxy matrices using carbon nanotubes masterbatch. *Composites Part A* **2014**, *61*, 126–133.
31. Prashantha, K.; Soulestin, J.; Lacrampe, M.F.; Krawczak, P.; Dupin, G.; Claes, M. Masterbatch-based multi-walled carbon nanotube filled polypropylene nanocomposites: Assessment of rheological and mechanical properties. *Compos. Sci. Technol.* **2009**, *69*, 1756–1763.
32. Al-Saleh, M.H.; Sundararaj, U. Electromagnetic interference shielding mechanisms of CNT/polymer composites. *Carbon* **2009**, *47*, 1738–1746.
33. Arjmand, M.; Apperley, T.; Okoniewski, M.; Sundararaj, U. Comparative study of electromagnetic interference shielding properties of injection molded *versus* compression molded multi-walled carbon nanotube/polystyrene composites. *Carbon* **2012**, *50*, 5126–5134.
34. Arjmand, M.; Mahmoodi, M.; Gelves, G.A.; Park, S.; Sundararaj, U. Electrical and electromagnetic interference shielding properties of flow-induced oriented carbon nanotubes in polycarbonate. *Carbon* **2011**, *49*, 3430–3440.
35. Cao, J.-P.; Zhao, J.; Zhao, X.; You, F.; Yu, H.; Hu, G.-H.; Dang, Z.-M. High thermal conductivity and high electrical resistivity of poly(vinylidene fluoride)/polystyrene blends by controlling the localization of hybrid fillers. *Compos. Sci. Technol.* **2013**, *89*, 142–148.

36. D'Aloia, A.G.; Marra, F.; Tamburrano, A.; de Bellis, G.; Sarto, M.S. Electromagnetic absorbing properties of graphene–polymer composite shields. *Carbon* **2014**, *73*, 175–184.
37. Mahmoodi, M.; Arjmand, M.; Sundararaj, U.; Park, S. The electrical conductivity and electromagnetic interference shielding of injection molded multi-walled carbon nanotube/polystyrene composites. *Carbon* **2012**, *50*, 1455–1464.
38. Thomassin, J.-M.; Jerome, C.; Pardoen, T.; Bailly, C.; Huynen, I.; Detrembleur, C. Polymer/carbon based composites as electromagnetic interference (EMI) shielding materials. *Mater. Sci. Eng. R* **2013**, *74*, 211–232.
39. Bian, J.; Lin, H.L.; He, F.X.; Wei, X.W.; Chang, I.T.; Sancaktar, E. Fabrication of microwave exfoliated graphite oxide reinforced thermoplastic polyurethane nanocomposites: Effects of filler on morphology, mechanical, thermal and conductive properties. *Composites Part A* **2013**, *47*, 72–82.
40. Deetuam, C.; Samthong, C.; Thongyai, S.; Praserthdam, P.; Somwangthanaroj, A. Synthesis of well dispersed graphene in conjugated poly(3,4-ethylenedioxythiophene):polystyrene sulfonate via click chemistry. *Compos. Sci. Technol.* **2014**, *93*, 1–8.
41. Garzon, C.; Palza, H. Electrical behavior of polypropylene composites melt mixed with carbon-based particles: Effect of the kind of particle and annealing process. *Compos. Sci. Technol.* **2014**, *99*, 117–123.
42. Noel, A.; Faucheu, J.; Rieu, M.; Viricelle, J.-P.; Bourgeat-Lami, E. Tunable architecture for flexible and highly conductive graphene–polymer composites. *Compos. Sci. Technol.* **2014**, *95*, 82–88.
43. Zhao, S.; Chen, F.; Zhao, C.; Huang, Y.; Dong, J.-Y.; Han, C.C. Interpenetrating network formation in isotactic polypropylene/graphene composites. *Polymer* **2013**, *54*, 3680–3690.